

The Others: Naturally Isolating Out-of-Distribution Samples for Robust Open-Set Semi-Supervised Learning

You Rim Choi¹ Subeom Park¹ Seojun Heo¹

Eunchung Noh² Hyung-Sin Kim^{*1}

Seoul National University¹ Samsung²

{yrchoi, sbpark7, seodalzzz, hyungkim}@snu.ac.kr
iameunchung@gmail.com

Abstract

Open-Set Semi-Supervised Learning (OSSL) tackles the practical challenge of learning from unlabeled data that may include both in-distribution (ID) and unknown out-of-distribution (OOD) classes. However, existing OSSL methods form suboptimal feature spaces by either excluding OOD samples, interfering with them, or overtrusting their information during training. In this work, we introduce MagMatch, a novel framework that naturally isolates OOD samples through a prototype-based contrastive learning paradigm. Unlike conventional methods, MagMatch does not assign any prototypes to OOD samples; instead, it selectively aligns ID samples with class prototypes using an ID-Selective Magnetic (ISM) module, while allowing OOD samples – the “others” – to remain unaligned in the feature space. To support this process, we propose Selective Magnetic Alignment (SMA) loss for unlabeled data, which dynamically adjusts alignment based on sample confidence. Extensive experiments on diverse datasets demonstrate that MagMatch significantly outperforms existing methods in both closed-set classification accuracy and OOD detection AUROC, especially in generalizing to unseen OOD data.

1. Introduction

Semi-supervised learning (SSL) leverages both a limited amount of labeled data and a larger volume of unlabeled data. Traditional SSL assumes that labeled and unlabeled data share the same set of classes, but this assumption is unrealistic, as real-world unlabeled data often contain unknown classes. Open-set SSL (OSSL) targets a more practical setting where the unlabeled dataset may include novel out-of-distribution (OOD) classes. An OSSL method must meet two key objectives: (1) accurately classify in-distribution (ID) data (i.e., closed-set classification) and (2) effectively detect OOD samples. Importantly, it must generalize beyond the limited OOD samples provided during training to identify

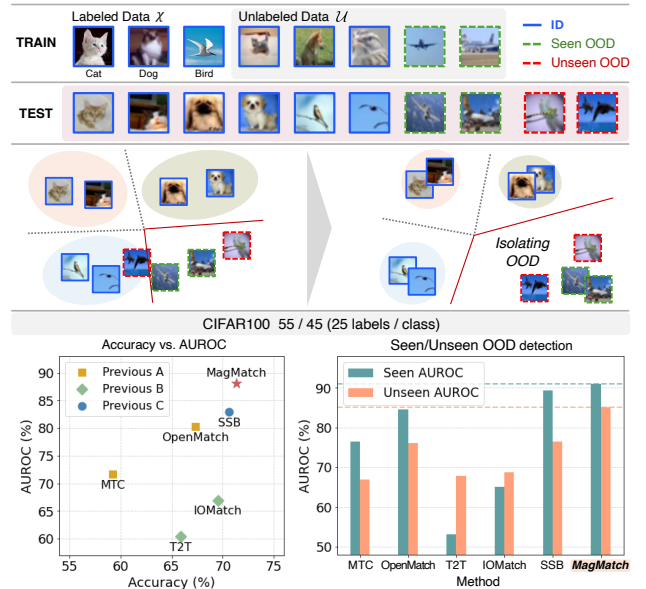


Figure 1. **Overview of Open-Set Semi-Supervised Learning (OSSL) and our approach.** In OSSL, unlabeled data contain novel classes (*seen OOD*) absent from labeled data, and the model must classify ID samples while detecting both seen and *unseen* OOD samples at test time. *MagMatch* enhances feature structuring by forming compact ID clusters and naturally distancing OOD samples, improving both seen and unseen OOD detection. Performance comparisons show *MagMatch* surpasses prior methods, especially in unseen OOD detection.

diverse, unseen OOD data from entirely novel distributions – an essential capability for real-world deployment.

Achieving these goals is challenging due to the complexity of utilizing unlabeled OOD samples during training. Early OSSL methods [4, 17, 26] treat OOD samples as harmful to closed-set classification and exclude them from training. However, this limits feature diversity and discards valuable information, leading to poorer ID class separation and weaker generalization to unseen OOD samples, as observed in Previous A of Figure 1. To better leverage OOD

data, some methods [8, 13, 20, 21] introduce auxiliary tasks, such as rotation prediction or open-set classification, to integrate OOD samples into representation learning. While these methods enhance ID class separability, they often blur ID-OOD boundaries, particularly when OOD samples closely resemble ID classes (e.g., ID: bird, OOD: airplane), as shown in Previous B of Figure 1. Other methods [3, 23] use confidence-based filtering to selectively retain useful OOD samples for the closed-set classifier while incorporating diverse OOD data to improve detection. Although these approaches enhance both classification and OOD detection, they tend to overfit the limited, seen OOD classes, restricting their ability to detect truly novel, unseen OOD samples, as illustrated in Previous C of Figure 1.

We propose *MagMatch*, an OSSL method that structures the feature space using class prototypes, promoting compact ID clusters while allowing OOD samples to remain naturally isolated. *MagMatch* consists of three components: a closed-set classifier, an OOD detector, and the ID-Selective Magnet (ISM) module, all sharing a unified feature extractor. Inspired by magnetic interactions, ISM treats class prototypes as magnets that selectively attract ID samples while leaving OOD samples unaffected – much like ferromagnetic materials attract while non-magnetic materials do not. Unlike previous approaches that either discard OOD samples or force them to predefined clusters (i.e., treating OOD as ferromagnetic materials), ISM focuses solely on aligning ID samples with their class prototypes, ensuring that ID features are compact and well-separated while OOD samples (i.e., non-magnetic materials) remain distinct naturally. This contrasts with prototypical contrastive learning (PCL) [12], which forces all unlabeled samples – including OOD samples – to align with learned prototypes, often misaligning OOD embeddings and distorting the feature space. By concentrating exclusively on ID alignment, ISM enhances class separability and maintains a structured feature space that generalizes effectively to unseen OOD samples.

The ISM module tackles three key challenges: (1) Minimizing interference with the main tasks: By operating in a separate low-dimensional projection space, ISM enhances representation learning without disrupting the closed-set classifier or the OOD detector. (2) Balancing reliance on limited labeled data: Rather than relying solely on labeled samples, ISM adaptively refines class prototypes by incorporating high-confidence ID samples from the unlabeled set. (3) Ensuring reliable alignment: Unlike PCL, which forces all unlabeled samples to align with prototypes, ISM selectively aligns only those samples that are confidently identified as ID, leaving OOD samples unaligned. This prevents misalignment and feature distortion, reducing overfitting to seen OOD and improving generalization to unseen OOD.

A core challenge in OSSL is determining which unlabeled samples should be aligned with class prototypes. To address

this, ISM introduces Selective Magnetic Alignment (SMA) Loss, which aligns unlabeled samples based on the agreement between the closed-set classifier and the OOD detector. For labeled samples, ISM applies Magnetic Alignment (MA) Loss, pulling each sample toward its class prototype to reinforce intra-class compactness. For unlabeled samples, Selective Magnetic Alignment (SMA) Loss dynamically selects ID samples using confidence thresholds. Confident ID samples are attracted to their class prototypes, while uncertain or OOD samples remain unaligned. This selective attraction mechanism prevents overfitting to seen OODs and ensures a well-structured feature space that generalizes to unseen OODs.

We evaluate *MagMatch* across diverse OSSL benchmarks, assessing performance using closed-set classification accuracy and AUROC for OOD detection. Unlike prior works that focus primarily on seen OOD detection, we systematically evaluate performance on both seen and unseen OOD samples to highlight generalization of our method. Our results consistently demonstrate state-of-the-art or near state-of-the-art performance, demonstrating the effectiveness of *MagMatch* in structuring the feature space while maintaining robustness to novel distributions.

2. Related Work

2.1. Open-set Semi-Supervised Learning (OSSL)

OSSL aims to improve closed-set classification while detecting OOD samples. Early methods focus on identifying and excluding OOD samples to minimize their impact on classification. MTC [26] employs Otsu thresholding, DS³L [4] applies meta-optimization, and OpenMatch [17] adopts a One-vs-All (OVA) classifier [16]. However, removing OOD samples often degrades closed-set accuracy compared to standard SSL.

To better utilize OOD data, recent methods integrate OOD samples into training. SSB [3] separates feature spaces for ID classification and OOD detection while leveraging reliable OOD samples as negatives for OOD detector training. SCOMatch [23] assigns high-confidence OOD samples to an additional class in a $(K + 1)$ -way classification setup. These approaches improve closed-set classification and OOD detection but tend to overfit seen OOD samples, limiting generalization to unseen OOD classes.

Other approaches introduce auxiliary tasks to enhance OOD representation learning. T2T [8] predicts image orientation, and SeFOSS [20] enforces feature consistency via cosine similarity. However, these tasks are not directly aligned with OSSL objectives, limiting their effectiveness. In contrast, IOMatch [13] introduces an open-set classifier to explicitly model OOD samples but suffers from noisy pseudo-labels. ProSub [21] defines ID feature centers as subspaces and applies a probabilistic model based on angular distances, incorporating a cosine similarity-based self-supervised loss

to better utilize OOD data. However, its reliance on a Beta distribution for subspace modeling may reduce its adaptability across different data configurations. These challenges highlight the difficulty of designing auxiliary tasks that enhance both closed-set classification and OOD detection without introducing additional limitations.

2.2. Contrastive Learning

To design an auxiliary task suited for OSSL, our *MagMatch* incorporates contrastive learning principles while addressing its limitations in the presence of OOD data. Traditional instance-level contrastive learning, often unsupervised [1, 6, 24], does not align well with OSSL objectives. It relies on instance-instance similarities, leading to false negative pairs and failing to leverage label information. SupCon [9] addresses these issues by using supervised labels to define positive and negative pairs, improving class separability. PCL [12] introduces prototype-based contrastive learning, where samples are pulled toward learned prototypes instead of individual instances. However, PCL does not distinguish between ID and OOD samples, forcing all unlabeled samples – including OOD – to align with one of the prototypes. This can distort the feature space by pulling OOD samples toward predefined groups, including ID clusters.

MagMatch’s ISM module addresses these limitations by selectively aligning only ID samples to class prototypes while preventing OOD samples from being forced into predefined clusters. By ensuring that ID samples form compact representations while allowing OOD samples to remain naturally unaligned, ISM enhances both ID classification and OOD detection without overfitting to seen OOD classes.

3. MagMatch

Problem Setting. For K -way classification, let $\mathcal{X} = \{(x_i, y_i) : i \in (1, \dots, B)\}$ be a batch of B labeled samples, where x_i is randomly sampled from the labeled training set \mathcal{D}_l , and $y_i \in (1, \dots, K)$ is the corresponding label. Let $\mathcal{U} = \{(u_i) : i \in (1, \dots, \gamma B)\}$ be a batch of γB samples from the unlabeled training set \mathcal{D}_u , where γ controls the labeled-to-unlabeled ratio. Unlike SSL, OSSL includes *OOD samples* from unknown classes in \mathcal{D}_u . Data augmentation consists of weak transformations $\mathcal{T}_w(\cdot)$, $\mathcal{T}_{w'}(\cdot)$ (without random cropping), and a strong transformation $\mathcal{T}_s(\cdot)$.

3.1. Overall Architecture

Our model, depicted in Figure 2, consists of a single feature extractor shared by three components. Given an input sample, the feature extractor outputs a shared embedding: for a labeled sample x_i^t , it produces $h_i^t \in \mathbb{R}^D$, and for an unlabeled sample u_i^t , it generates $h_{u,i}^t \in \mathbb{R}^D$, where $t \in \{w, w', s\}$ denotes the augmentation type. These embeddings serve as input to each component. Each of the three components is optimized for its respective task:

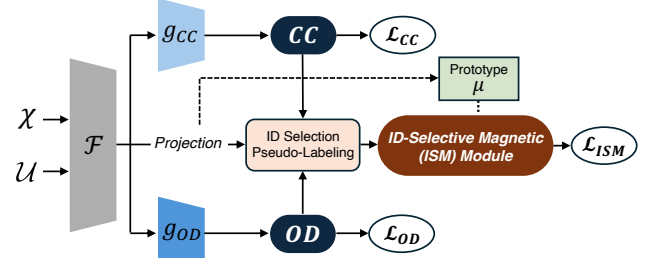


Figure 2. **Overall Architecture of *MagMatch*.** MLP layers, $g_{CC}(\cdot)$ and $g_{OD}(\cdot)$, are added before each task head to mitigate inter-head interference. The ID-Selective Magnetic (ISM) Module applies an additional MLP projection to shared encoder features, ensuring a lower-dimensional representation while minimizing interference. The $CC(\cdot)$ and $OD(\cdot)$ functions facilitate ID selection and pseudo-labeling, supporting the ISM Module.

- **Closed-set classifier ($CC(\cdot)$)** handles ID K -class classification, producing a probability vector $\mathbf{p} \in \mathbb{R}^K$. It is trained using labeled data and a subset of unlabeled data that are confidently pseudo-labeled as ID samples, filtered based on softmax thresholds.
- **OOD detector ($OD(\cdot)$)** distinguishes between ID and OOD using a one-vs-all (OVA) classifier composed of K sub-classifiers. It is trained using labeled ID samples and unlabeled samples confidently identified as OOD.
- **ID-Selective Magnet (ISM) module**, the core of *MagMatch*, structures the feature space to improve both closed-set classification and OOD detection while ensuring generalization to unseen OODs. Inspired by magnetic interactions, ISM treats class prototypes as magnets (attractors) that selectively pull ID samples while leaving OOD samples unaligned. This naturally structures the feature space by reinforcing ID compactness while allowing OOD to separate without explicit repulsion. ISM addresses three key challenges: (1) Minimizing interference with main tasks by operating in a lower-dimensional projection space with an added non-linearity, preventing ISM from directly altering shared feature representations, (2) Refining prototypes adaptively by incorporating reliable ID samples from unlabeled data, and (3) Ensuring reliable alignment by selectively pulling only confident ID samples.

3.2. Feature Adaptation for Task-Specific Learning

The ISM module, when added as an auxiliary task, may interfere with the two main tasks due to the shared feature extractor. To mitigate this, we introduce task-specific adaptation via non-linear transformations, ensuring that each component learns representations tailored to its objective.

Closed-set classification requires embeddings that distinctly separate ID classes, while OOD detection focuses on distinguishing ID from OOD samples. To facilitate this, we apply an MLP layer before each task head, allowing the closed-set classifier ($CC(\cdot)$) and OOD detector ($OD(\cdot)$) to specialize their embeddings independently. Similarly, the

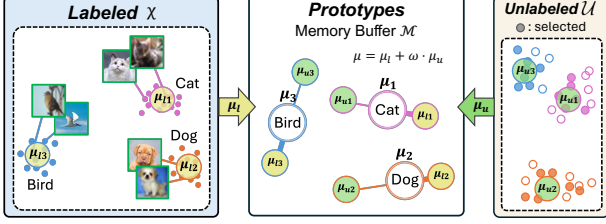


Figure 3. **Adaptive Magnet Generation.** Each labeled prototype μ_l is the mean embedding of labeled data for each class, while the unlabeled prototype μ_u is obtained from the mean embedding of confident ID data among the unlabeled data. The final magnetic prototype μ is produced as a weighted sum of these two prototypes.

ISM module applies a separate MLP projection, ensuring that it operates in a distinct lower-dimensional space rather than directly modifying the shared feature representations. This projection prevents ISM from interfering with other task-specific feature adaptation while simultaneously enhancing the shared feature space to better structure ID clusters and naturally separate OOD samples. By selectively aligning ID samples with their class prototypes, ISM reinforces the shared encoder’s ability to learn compact, well-separated ID representations, which in turn benefits both closed-set classification and OOD detection. This structured feature space improves generalization not only within ID classes but also for unseen OOD samples. Given a labeled embedding h_i^t , we obtain:

- **Closed-set classification output:** $\mathbf{p}_i^t \in \mathbb{R}^K$, a softmax probability vector over the K ID classes.
- **OOD detection output:** $\varphi_i^t \in \mathbb{R}^{2K}$, where each class-specific binary classifier $OD_k(\cdot)$ predicts the likelihood of ID vs. OOD.
- **ISM module projection:** $z_i^t = \text{proj}(h_i^t) \in \mathbb{R}^d$, ensuring a structured, independent representation for alignment.

For an unlabeled sample $h_{u,i}^t$, the same transformation process is applied, producing $\mathbf{p}_{u,i}^t$, $\varphi_{u,i}^t$, and $z_{u,i}^t$. By decoupling task-specific representations, our design prevents interference while allowing each component to optimize for its respective goal.

3.3. Magnetic Prototype Refinement

Unlike instance-wise contrastive learning, which suffers from false negative pairs [15], *MagMatch* employs a prototype-based approach where each of the K ID classes is represented by a prototype that serves as its central embedding. To ensure stable training, class-wise prototypes are computed in an EMA manner, ensuring smooth transitions across training iterations [11]. These prototypes act as magnetic attractors, guiding ID embeddings toward class centers while leaving OOD samples unaligned. OOD samples exhibit high heterogeneity and do not form stable clusters; thus, we do not construct prototypes for them, effectively treating them as non-magnetic materials.

Initially, we compute a labeled prototype μ_{lk} for each

class k by averaging low-dimensional embeddings $z_i^w = \text{proj}(h_i^w)$ from weakly augmented labeled samples. However, relying solely on labeled data may lead to suboptimal prototypes, as labeled data is significantly limited. To refine prototype estimation, *MagMatch* dynamically incorporates reliable ID samples from the unlabeled set throughout training. Using both $CC(\cdot)$ and $OD(\cdot)$, we select confident ID samples and compute their mean embedding μ_{uk} . The final prototype μ_k is obtained by weighting μ_{lk} and μ_{uk} based on their respective sample contributions, as illustrated in Figure 3. For a detailed explanation of the weighting process, refer to the Supplementary material. This adaptive process enhances the stability and discriminability of prototypes, reinforcing class-wise compactness while naturally maintaining ID-OOD separation.

3.4. ID-Selective Magnetic Learning

The ISM module structures the embedding space by enhancing intra-class compactness while preserving a structured separation between ID and OOD samples without introducing artificial distortions. Rather than enforcing explicit repulsion or forcing OOD samples into predefined clusters, ISM organizes the feature space through *selective attraction*: ID embeddings are drawn toward their respective prototypes, while non-ID embeddings remain unaffected.

3.4.1. Alignment Loss for Labeled Data

For labeled samples, we define positive and negative pairs using ground-truth labels, enabling direct supervision for learning discriminative representations. To fully utilize this supervision, we apply both Instance-wise Alignment (IA) loss and Magnetic Alignment (MA) loss, each reinforcing intra-class compactness while indirectly promoting inter-class separation.

The Instance-wise Alignment (IA) loss, inspired by SupCon [9], encourages embeddings of the same class to cluster together:

$$\mathcal{L}_{\text{IA}}(z_i^w) := \frac{1}{|P(i)|} \sum_{p \in P(i)} \log \frac{\exp(z_i^w \cdot z_p^w / T)}{\sum_{j=1}^B \mathbb{1}_{i \neq j} \exp(z_i^w \cdot z_j^w / T)} \quad (1)$$

where $P(i)$ denotes the set of sample indices belonging to the same class as sample i (y_i), excluding i itself. T is a temperature parameter that adjusts distribution sharpness.

To further enhance intra-class compactness, we introduce the Magnetic Alignment (MA) loss, a magnet-based adaptation of InfoNCE loss [15], which attracts ID embeddings toward their respective class prototypes:

$$\mathcal{L}_{\text{MA}}(z_i^w) := - \frac{z_i^w \cdot \mu_{y_i} / T}{\log \sum_{j=1}^K \exp(z_i^w \cdot \mu_j / T)} \quad (2)$$

where μ_{y_i} is the prototype of class y_i .

MA loss optimizes embeddings of labeled ID samples by maximizing their magnetic pull toward the corresponding

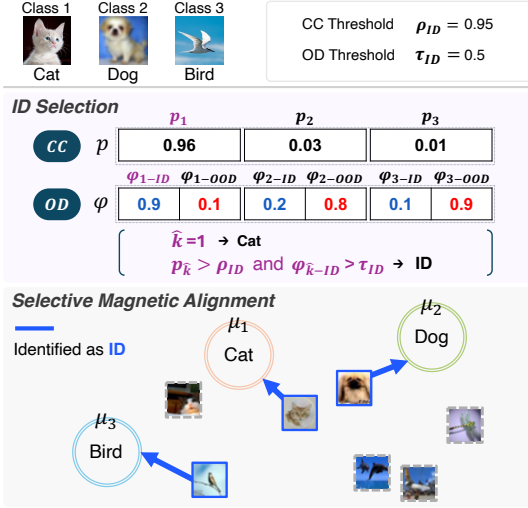


Figure 4. **ID Selection and Selective Magnetic Alignment.** The ID Selection process determines whether an unlabeled sample is ID based on $CC(\cdot)$ confidence (p_k) and $OD(\cdot)$ score (φ_k). A sample is classified as ID if $p_{\hat{k}} > \rho_{ID}$ and $\varphi_{\hat{k}-ID} > \tau_{ID}$. In Selective Magnetic Alignment, only confidently identified ID samples are attracted toward their respective class prototypes.

class prototype while contrasting them against all class prototypes in the denominator. Although MA does not explicitly repel embeddings from other prototypes, this contrastive formulation naturally strengthens ID clusters while relatively distancing them from others—akin to a selective magnetic attraction where ID samples are drawn to their prototype, while non-matching samples remain non-magnetic. As a result, a structured feature space emerges, benefiting both ID classification and OOD detection.

3.4.2. Selective Magnetic Alignment Loss

Unlabeled data introduce inherent uncertainty in OSSS due to the presence of OOD samples and the absence of ground-truth labels. To ensure that only reliable ID samples are aligned with class prototypes while non-ID samples remain unaligned, the ISM module selectively applies magnetic attraction based on the agreement between the closed-set classifier and the OOD detector.

For an unlabeled embedding $z_{u,i}^w$, we determine its ID confidence for its predicted class \hat{k} using a confidence mask $\Phi_{u,i}$, defined as:

$$\Phi_{u,i} = \mathbb{1} \left(p_{u,i,\hat{k}}^w > \tau_{ID} \text{ and } \varphi_{u,i,\hat{k}-ID}^{w'} > \eta_{ID} \right) \quad (3)$$

where τ_{ID} and η_{ID} are confidence thresholds for class prediction (closed-set classifier) and ID detection (OOD detector). The dominant class, defined as $\hat{k} = \arg \max_k p_{u,i,k}^w$, is the class with the highest predicted probability. For confidently classified unlabeled ID samples, the corresponding class prototype $\mu_{\hat{k}}$ acts as a magnetic anchor, ensuring stable alignment.

The Selective Magnetic Alignment (SMA) loss extends the Magnetic Alignment (MA) loss by selectively aligning only confident ID samples to class prototypes:

$$\mathcal{L}_{SMA}(z_{u,i}^w) := -\Phi_{u,i} \frac{z_{u,i}^w \cdot \mu_{\hat{k}}/T}{\log \sum_{j=1}^K \exp(z_{u,i}^w \cdot \mu_j/T)} \quad (4)$$

By restricting magnetic alignment to only confidently considered ID samples, SMA prevents unreliable pseudo-labels from distorting the feature space. Unlike standard contrastive losses that either force all unlabeled samples into clusters or explicitly repel OOD samples, SMA enables a natural structuring of ID and OOD embeddings through selective attraction. This mechanism enhances class separability while mitigating overfitting to seen OODs, ultimately improving generalization to unseen OOD samples. Through this, regardless of whether the model has seen the class during training (Seen) or not (Unseen), *MagMatch* can handle the remaining “The Others” as OOD without being pulled.

3.5. Objectives

In this section, we detail the objective function used to train the entire framework.

Closed-set classifier. The closed-set classifier is trained following the pseudo-labeling framework of FixMatch [18], which encourages consistency between weakly and strongly augmented views using confidence-based pseudo-labels. The classification loss \mathcal{L}_{cc} consists of a supervised loss \mathcal{L}_x for labeled samples and an unsupervised loss \mathcal{L}_u for unlabeled samples. For labeled samples in \mathcal{X} , we apply the standard cross-entropy loss using weak augmentations w and w' . For unlabeled samples in \mathcal{U} , we generate pseudo-labels from weak augmentations and enforce consistency with their strongly augmented counterparts. Only high-confidence pseudo-labels are retained, preventing noisy supervision.

OOD detector. The OOD detector adopts the loss functions proposed in OVANet [16] and OpenMatch [17]. For labeled samples, it applies the One-vs-All (OVA) loss $\mathcal{L}_{od}^{OVA}(\mathcal{X})$, where the assigned class is treated as positive (ID) and all others as negative (OOD) using binary cross-entropy. For unlabeled samples, it employs an entropy minimization loss $\mathcal{L}_{od}^{em}(\mathcal{U})$ to enhance ID-OOD separation, along with a soft open-set consistency regularization loss $\mathcal{L}_{od}^{SOCR}(\mathcal{U})$, which enforces consistency between two weak augmentations, $\varphi_{u,i,k}^w$ and $\varphi_{u,i,k}^{w'}$. Standard OVA loss does not utilize unlabeled data. However, to improve ID-OOD separation, we introduce an additional negative loss \mathcal{L}_{od}^{neg} , inspired by pseudo-negative mining in SSB [3]. This loss incorporates confidently identified OOD samples from the unlabeled set, encouraging the model to classify them more distinctly as OOD. Unlike prior methods, we apply weak and strong augmentations to negative samples from both labeled and unlabeled data, further enhancing robustness.

The final OOD detector loss is defined as:

Table 1. Closed-set classification accuracy (Acc.) and OOD detection AUROC on CIFAR-10 and CIFAR-100 across different datasets, ID class distributions, and labeled data settings. The mean and standard deviation were reported based on three experiments with a fixed random seed. For each setting, the best performance is highlighted in **bold**, while the second-best performance is underlined.

Dataset	CIFAR-10 6/4				CIFAR-100 55/45				CIFAR-100 80/20				ImageNet30	
	25		50		25		50		25		50		5%	
	Acc.	AUROC	Acc.	AUROC	Acc.	AUROC	Acc.	AUROC	Acc.	AUROC	Acc.	AUROC	Acc.	AUROC
MTC [26]	71.73 ±11.01	85.46 ±6.08	80.95 ±5.33	92.11 ±2.7	59.23 ±1.98	71.68 ±1.32	66.03 ±0.75	69.38 ±1.17	52.92 ±0.15	67.53 ±0.72	59.68 ±0.03	69.29 ±3.33	80.77 ±0.66	80.9 ±2.53
OpenMatch [17]	65.94 ±1.96	53.93 ±4.46	90.50 ±1.16	95.79 ±0.59	67.29 ±1.32	80.28 ±0.12	71.84 ±1.15	83.05 ±0.53	52.65 ±4.51	68.57 ±4.20	67.05 ±0.23	80.30 ±0.35	79.04 ±0.40	83.67 ±0.09
T2T [8]	83.66 ±0.88	47.22 ±15.89	90.78 ±0.06	41.15 ±9.77	65.91 ±0.87	60.45 ±2.94	70.81 ±0.11	62.28 ±1.21	48.01 ±9.89	52.02 ±5.25	64.14 ±0.54	68.06 ±8.52	89.02 ±0.95	72.88 ±1.25
IOMatch [13]	93.77 ±0.18	53.19 ±1.50	93.37 ±0.40	48.10 ±1.77	69.52 ±0.50	66.95 ±1.7	73.23 ±0.04	68.23 ±1.13	64.81 ±0.49	65.33 ±1.44	68.56 ±0.13	61.06 ±2.04	84.49 ±0.33	70.52 ±2.31
SSB [3]	91.74 ±0.24	<u>95.86</u> ±1.37	92.18 ±0.33	<u>97.65</u> ±0.19	<u>70.64</u> ±0.36	<u>82.90</u> ±0.30	<u>73.70</u> ±0.75	<u>85.89</u> ±0.07	64.20 ±0.41	<u>81.71</u> ±0.86	67.97 ±0.20	80.81 ±1.02	91.80 ±0.05	82.80 ±1.18
ProSub [21]	88.03 ±0.97	93.64 ±0.38	88.51 ±2.08	93.09 ±1.27	63.65 ±0.99	76.41 ±2.82	69.16 ±1.39	80.76 ±0.59	55.21 ±1.12	78.90 ±3.04	61.14 ±1.92	<u>83.98</u> ±1.24	<u>91.43</u> ±0.75	<u>92.17</u> ±4.39
MagMatch	<u>92.04</u> ±0.23	98.12 ±0.16	<u>93.24</u> ±0.18	98.41 ±0.24	71.32 ±0.22	88.10 ±0.42	74.95 ±0.45	89.33 ±0.18	67.18 ±0.21	87.88 ±0.09	70.28 ±0.18	88.75 ±0.11	91.20 ±0.15	92.72 ±0.22

Table 2. AUROC performance comparison for Seen and Unseen OOD across different datasets and label settings.

Dataset	CIFAR-10 6/4				CIFAR-100 55/45				CIFAR-100 80/20				ImageNet30	
	25		50		25		50		25		50		5%	
	Seen	Unseen	Seen	Unseen	Seen	Unseen	Seen	Unseen	Seen	Unseen	Seen	Unseen	Seen	Unseen
MTC [26]	91.98 ±3.20	78.94 ±8.95	94.27 ±1.95	89.95 ±3.45	76.50 ±1.38	66.85 ±1.25	72.95 ±0.32	65.80 ±2.02	69.11 ±1.43	65.95 ±0.01	71.98 ±2.24	66.60 ±5.20	82.80 ±2.45	79.0 ±1.88
OpenMatch [17]	63.01 ±3.99	44.85 ±5.35	99.33 ±0.15	92.25 ±1.02	84.53 ±0.08	76.02 ±0.15	87.13 ±0.25	78.96 ±0.80	75.02 ±3.91	62.12 ±4.67	86.69 ±0.68	73.90 ±0.08	91.58 ±0.46	75.76 ±0.64
T2T [8]	38.22 ±22.00	56.22 ±9.78	24.95 ±10.32	57.34 ±9.21	53.10 ±5.45	67.84 ±0.42	59.70 ±1.82	64.86 ±0.60	50.25 ±8.92	53.78 ±0.56	67.21 ±15.50	68.91 ±6.74	63.44 ±2.08	82.32 ±0.52
IOMatch [13]	46.57 ±1.32	49.81 ±1.67	47.32 ±1.49	48.88 ±2.05	65.10 ±1.07	68.80 ±2.33	66.73 ±1.72	69.72 ±0.54	64.94 ±1.56	65.71 ±1.22	60.01 ±1.72	62.11 ±2.40	69.56 ±1.96	71.48 ±2.55
SSB [3]	<u>99.35</u> ±0.38	92.37 ±2.36	99.63 ±0.15	<u>95.67</u> ±0.23	<u>89.39</u> ±0.44	<u>76.44</u> ±0.15	90.62 ±0.46	<u>81.16</u> ±0.61	<u>90.25</u> ±1.34	73.18 ±0.38	85.29 ±2.18	<u>76.34</u> ±0.14	83.84 ±2.31	81.77 ±0.04
ProSub [21]	88.03 ±0.97	<u>93.64</u> ±0.38	88.51 ±2.08	93.09 ±1.27	63.65 ±0.99	76.41 ±2.82	69.16 ±1.39	80.76 ±0.59	55.21 ±1.12	<u>78.90</u> ±3.04	<u>92.33</u> ±2.90	75.62 ±4.15	97.74 ±0.26	86.60 ±8.88
MagMatch	99.39 ±0.15	96.84 ±0.21	<u>99.31</u> ±0.18	97.50 ±0.19	91.09 ±0.41	85.11 ±0.50	<u>90.23</u> ±0.16	88.43 ±0.20	91.86 ±0.23	83.90 ±0.15	92.32 ±0.24	85.17 ±0.22	<u>95.53</u> ±0.33	89.90 ±0.45

$$\mathcal{L}_{\text{od}} = \mathcal{L}_{\text{od}}^{\text{OVA}}(\chi) + \lambda_{\text{em}} \mathcal{L}_{\text{od}}^{\text{em}}(\mathcal{U}) + \lambda_{\text{SOCR}} \mathcal{L}_{\text{od}}^{\text{SOCR}}(\mathcal{U}) + \lambda_{\text{neg}} \mathcal{L}_{\text{od}}^{\text{neg}}(\mathcal{U}) \quad (5)$$

ISM Module. The total ISM loss \mathcal{L}_{ISM} , combining instance-wise alignment and magnet-based alignment for both labeled and unlabeled data, is defined as:

$$\mathcal{L}_{\text{ISM}} = \lambda_{\text{IA}} \mathcal{L}_{\text{IA}}(\chi) + \lambda_{\text{MA}} \mathcal{L}_{\text{MA}}(\chi) + \lambda_{\text{SMA}} \mathcal{L}_{\text{SMA}}(\mathcal{U}) \quad (6)$$

where λ_{IA} , λ_{MA} , and λ_{SMA} are weighting factors controlling the contribution of each loss term.

Overall Objective. The overall objective of *MagMatch* is:

$$\mathcal{L}_{\text{Total}} = \lambda_{\text{cc}} \mathcal{L}_{\text{cc}} + \lambda_{\text{od}} \mathcal{L}_{\text{od}} + \lambda_{\text{ISM}} \mathcal{L}_{\text{ISM}} \quad (7)$$

4. Experiments

4.1. Experimental Setup

Setup. We evaluate *MagMatch* following the standard experimental settings in OSSL research. For the CIFAR-10 [10] and CIFAR-100 [10] datasets, we use WideResNet-28-2 [27] as the shared feature extractor, and conduct experiments by varying the number of ID/OOD classes and the amount of labeled data. For ImageNet [2], we evaluate on a subset consisting of 30 classes, referred to as ImageNet30 [7], using ResNet18 [5] as the feature extractor, consistent with prior works. Our implementation is based on the USB code-base [22]. The CIFAR-10 experiments were conducted on

a single NVIDIA H100 GPU, while all other experiments were run on four NVIDIA RTX 3090 GPUs.

Baselines. We compare *MagMatch* with several existing OSSL methods. MTC [26] and OpenMatch [17] focus on filtering out OOD data to reduce their negative impact. Notably, OpenMatch introduces the OVA-Classifier, which we also use as our OOD detector. T2T [8], IOMatch [13], SSB [3], and ProSub [21] instead leverage OOD data to improve classification and OOD detection, each employing different strategies. For a fair comparison, all methods were evaluated under the same dataset and experimental settings based on their original implementations, with SSB compared using its FixMatch-based results reported in the original paper.

Evaluation. We follow standard OSSL evaluation metrics, assessing both classification and OOD detection performance. For ID samples, we report classification accuracy, while OOD detection is evaluated using AUROC (Area Under the Receiver Operating Characteristic curve). The OOD set includes both seen OOD (encountered during training) and unseen OOD (not used during training). Unseen OOD detection is evaluated on CIFAR-10, CIFAR-100, ImageNet, LSUN [25], and SVHN [14]. Specifically, CIFAR-100 serves as the unseen OOD set for CIFAR-10, CIFAR-10 for CIFAR-100, and both CIFAR-10 and CIFAR-100 for ImageNet-30. All results are averaged over three runs, with

mean AUROC computed as the mean of seen and unseen OOD detection scores.

4.2. Main Results

Performances. For CIFAR-10, six animal classes are categorized as ID classes, while the remaining four classes are designated as OOD. In CIFAR-100, we first separate the classes based on their super-classes to ensure that ID and OOD classes do not overlap within the same super-class. We then further split these super-classes into ID and OOD groups. To examine the effects of varying OOD quantities, we evaluate two scenarios: one with 55 ID and 45 OOD classes, and another with 80 ID and 20 OOD classes. For each dataset configuration, we conduct experiments with 25 and 50 labeled samples per class. For ImageNet30, we divide the classes into 20 ID and 10 OOD classes, using 5% of the data (65 samples per class) as labeled data for our experiments.

Table 1 presents closed-set accuracy and mean AUROC across all data configurations, while Table 2 details Seen and Unseen AUROC. For CIFAR-10 and CIFAR-100, *MagMatch* achieves the highest mean AUROC and leads in accuracy for most cases, ranking second only on CIFAR-10. Importantly, *MagMatch* uniquely excels in both accuracy and AUROC across all settings. A key observation is that *MagMatch* demonstrates strong performance in Seen AUROC, achieving the best results in most cases, while significantly outperforming all baselines in Unseen AUROC across all datasets. This highlights *MagMatch*’s ability to prevent overfitting to Seen OOD samples, instead structuring the feature space such that OOD samples naturally separate from ID regions, leading to better generalization to Unseen OODs.

Another noteworthy aspect is the robustness of *MagMatch* across different number of labels. Unlike most baselines, which exhibit a substantial performance gap between 25-label and 50-label settings, *MagMatch* maintains consistently high AUROC across both, demonstrating its stability under varying supervision levels. On ImageNet-30, *MagMatch* maintains strong performance across accuracy, Seen AUROC, Unseen AUROC, and mean AUROC.

4.3. Feature Embedding Analysis

Shared Features. We analyzed the shared feature embeddings of models trained on CIFAR-10. Figure 5a presents t-SNE [19] visualizations of embeddings for 6 ID classes, Seen OOD, and Unseen OOD data. FixMatch, a standard SSL method, shows OOD samples clustering near the center, with some Seen OODs overlapping ID classes. OpenMatch, which aggressively filters OOD samples, also results in OODs clustering centrally but with numerous ID samples misclassified as OOD, contributing to its lower closed-set accuracy. IOMatch employs an OVA-classifier for OOD detection and an auxiliary open-set classifier, resulting in Seen OOD samples forming a few distinct clusters. However,

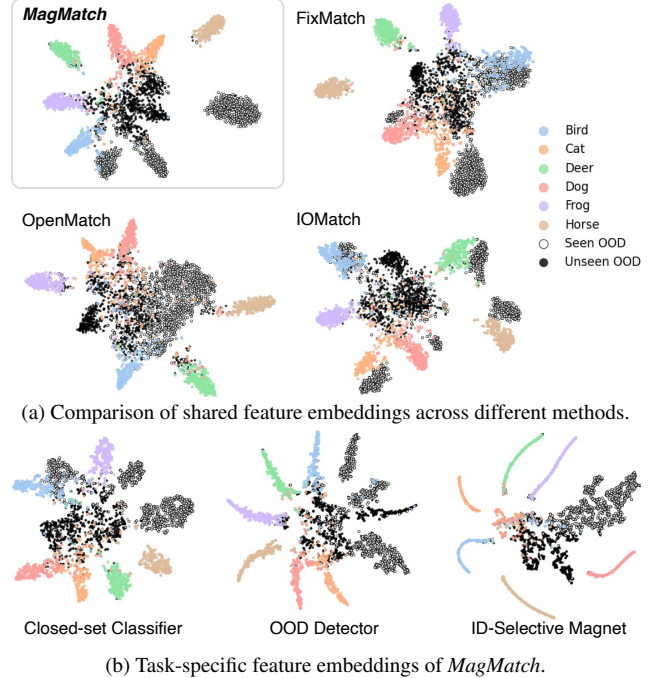


Figure 5. **Feature Embedding Analysis (CIFAR-10 6/4).** Compared to other methods, *MagMatch* forms compact class-wise clusters while naturally isolating OOD samples, ensuring clear ID-OD separation. The ID-Selective Magnet module aligns ID data around class prototypes, while OOD data remain in a separate space.

some ID-like OODs mix with ID samples, possibly due to incorrect pseudo-labeling in the open-set classifier.

In contrast, *MagMatch* produces well-structured embeddings with compact, well-separated ID clusters. Seen OOD samples are not only distinct from ID classes but also align in a single opposing direction, unlike other methods that disperse them randomly. Unseen OODs primarily appear near the boundary between ID and Seen OOD samples, maintaining clear separation from ID classes while exhibiting a radial trend extending toward the Seen OOD direction. Overall, OOD samples remain *isolated* in distinct regions, while ID clusters are well-formed with strong intra-class compactness.

Task-specific Features. In *MagMatch*, $CC(\cdot)$, $OD(\cdot)$, and the ISM module each play distinct roles, collectively shaping the shared feature space. Figure 5b presents visualizations of the corresponding embeddings. The $CC(\cdot)$ focuses on ID class discrimination, forming well-separated ID clusters. Similar to *FixMatch*, some Seen OOD samples partially overlap with ID embeddings, likely because they are treated as augmented data points for ID classes. In contrast, $OD(\cdot)$ clusters OOD samples in a distinct region, positioned opposite to the ID clusters along the overall radial pattern. The ISM module aligns ID embeddings toward class prototypes, forming compact yet structured clusters. This selective alignment process causes ID samples to arrange in elongated, snake-like patterns as they are gradually pulled toward their

Table 3. Performance comparison with different combinations of ISM loss components (CIFAR-100 80/20, 25 labels).

Exp. ID	Loss Combination			Accuracy	AUROC		
	IA	MA	SMA		Mean	Seen	Unseen
1				64.86	82.53	88.83	76.23
2	✓	✓		67.22	87.01	91.46	82.54
3			✓	67.18	87.25	89.88	84.61
4	✓	✓	✓	66.86	87.91	91.65	84.16
5	✓	✓	✓	67.26	88.79	91.86	85.71

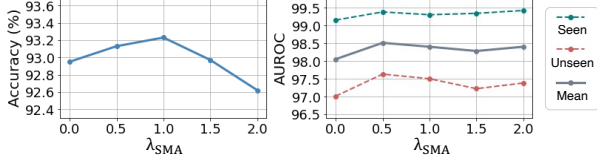


Figure 6. Effect of varying on weight of SMA loss (CIFAR-100 80/20, 25 labels).

Table 4. Impact of Task specific feature adaptation (CIFAR100 55/45, 25 labels).

Exp. ID	MLP layer			Accuracy	AUROC		
	CC	OD	ISM		Mean	Seen	Unseen
1				70.45	86.33	88.31	84.35
2	✓	✓		71.27	86.29	89.49	83.10
3			✓	71.02	86.43	88.95	83.91
4	✓	✓	✓	72.02	87.67	90.76	84.57

respective prototypes. Since OOD samples are not confidently identified as ID, they remain unaffected by this alignment, forming relatively dispersed but distinct clusters away from ID regions. This structured feature space helps *MagMatch* maintain clear ID-OOD separation while improving robustness against ambiguous samples.

4.4. Ablation

Loss Combination. Table 3 presents the results of experiments with different combinations of \mathcal{L}_{ISM} . Exp.2 shows that learning compact embeddings via \mathcal{L}_{IA} and \mathcal{L}_{MA} enhances ID/OOD discrimination. Exp.3 demonstrates that \mathcal{L}_{SMA} effectively improves Unseen AUROC by leveraging confident ID samples from unlabeled data. However, excluding any of these losses results in suboptimal performance, while Exp.5, which incorporates all, achieves the best performance in both Accuracy and AUROC. The improved ID/OOD discrimination through \mathcal{L}_{IA} and \mathcal{L}_{MA} contributes to stronger prototype formation, which, when combined with \mathcal{L}_{SMA} , creates a synergistic effect. This highlights the importance of integrating \mathcal{L}_{IA} , \mathcal{L}_{MA} , and \mathcal{L}_{SMA} for optimal performance.

Weight of SMA Loss. To further investigate the effect of \mathcal{L}_{SMA} , we analyze the impact of its weight, λ_{SMA} (Figure 6). Setting λ_{SMA} between 0.5 and 1 balances accuracy and AUROC. Increasing λ_{SMA} beyond this range slightly degrades both metrics, particularly accuracy. When λ_{SMA} becomes too large, the model places greater emphasis on unlabeled data, which may amplify the influence of uncertain pseudo-labels. Tuning λ_{SMA} within a moderate range maintains a balance between alignment and generalization.

Task-Specific Feature Adaptation. To investigate the effect of task-specific feature adaptation, we analyze the impact of adding the MLP layer in front of the Closed-set

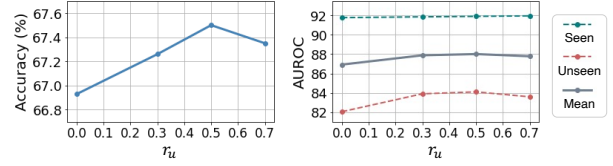


Figure 7. *MagMatch* performance with varying contribution ratios of unlabeled data (r_u) in prototype generation (CIFAR-100 55/45, 25 labels).

Table 5. Experimental results with different OD thresholds.

η_{ID}	CIFAR10 6/4 (50 labels)				CIFAR100 55/45 (25 labels)			
	Acc.	AUROC			Acc.	AUROC		
		Mean	Seen	Unseen		Mean	Seen	Unseen
0.3	92.05	98.15	99.33	96.96	71.81	86.52	89.77	83.26
0.5	93.23	98.40	99.28	97.51	71.78	87.11	90.70	83.51
0.7	<u>93.07</u>	<u>98.39</u>	99.35	<u>97.44</u>	72.02	87.67	90.76	84.57

Classifier (CC), OOD Detector (OD), and ISM module. Table 4 shows that adding MLP layers before CC and OD enhances both Accuracy and Seen AUROC. Adding an MLP layer to the ISM module (Exp.4) further improves Accuracy and Seen AUROC, with a significant boost in Unseen AUROC. This result demonstrates that incorporating MLP layers before each module effectively adapts the feature space to task-specific requirements, minimizing interference between modules and improving overall performance.

Magnetic Prototype Refinement. Figure 7 evaluates the effect of the contribution ratio of unlabeled data (r_u) when generating magnetic prototypes. Incorporating ID-selected unlabeled samples leads to more reliable and generalized prototypes compared to relying solely on labeled data ($r_u = 0$), improving Accuracy and AUROC, with a particularly noticeable enhancement in Unseen AUROC.

ID Selection Threshold. Selective magnetic alignment uses both the CC threshold (τ_{ID}) and the OD threshold (η_{ID}) for ID selection. The CC threshold is set to 0.99 with sharpening applied using a temperature of 0.5. Table 5 shows the results of experiments varying η_{ID} . Using the common binary classification threshold of 0.5 as a baseline, we compare lower and higher values. Setting η_{ID} to 0.3 degrades performance, suggesting unstable learning. This occurs because a lower threshold misclassifies more OOD samples as ID, pulling them toward ID prototypes and disrupting the feature space. Increasing η_{ID} to 0.7 improves performance on CIFAR-100 but slightly reduces accuracy on CIFAR-10, likely due to the difficulty in distinguishing similar ID classes like dogs and cats. Consequently, $\varphi_{u,i,\hat{k}-ID}^{w'}$ decreases, reducing the contribution of unlabeled ID samples. Overall, setting η_{ID} above 0.5 ensures more stable learning.

5. Conclusion

In this paper, we introduced *MagMatch*, a novel framework for OSSS that effectively structures the feature space to improve both closed-set classification and OOD detection. Unlike existing methods that attempt to assign OOD samples to specific classes or clusters, *MagMatch* naturally isolates OOD samples by selectively aligning only confident ID sam-

ples with class prototypes using ISM module. This design, guided by our proposed SMA loss, prevents overfitting to Seen OOD samples while enhancing generalization to Unseen OODs. Extensive experiments demonstrate that *Mag-Match* consistently achieves superior performance across various datasets and label configurations, offering a robust and effective solution for OSSL challenges.

References

- [1] Ting Chen, Simon Kornblith, Mohammad Norouzi, and Geoffrey Hinton. A simple framework for contrastive learning of visual representations. In *International conference on machine learning*, pages 1597–1607. PmLR, 2020. 3
- [2] Jia Deng, Wei Dong, Richard Socher, Li-Jia Li, Kai Li, and Li Fei-Fei. Imagenet: A large-scale hierarchical image database. In *2009 IEEE conference on computer vision and pattern recognition*, pages 248–255. Ieee, 2009. 6
- [3] Yue Fan, Anna Kukleva, Dengxin Dai, and Bernt Schiele. Ssb: Simple but strong baseline for boosting performance of open-set semi-supervised learning. In *Proceedings of the IEEE/CVF International Conference on Computer Vision*, pages 16068–16078, 2023. 2, 5, 6
- [4] Lan-Zhe Guo, Zhen-Yu Zhang, Yuan Jiang, Yu-Feng Li, and Zhi-Hua Zhou. Safe deep semi-supervised learning for unseen-class unlabeled data. In *International conference on machine learning*, pages 3897–3906. PMLR, 2020. 1, 2
- [5] Kaiming He, Xiangyu Zhang, Shaoqing Ren, and Jian Sun. Deep residual learning for image recognition. In *Proceedings of the IEEE conference on computer vision and pattern recognition*, pages 770–778, 2016. 6
- [6] Kaiming He, Haoqi Fan, Yuxin Wu, Saining Xie, and Ross Girshick. Momentum contrast for unsupervised visual representation learning. In *Proceedings of the IEEE/CVF conference on computer vision and pattern recognition*, pages 9729–9738, 2020. 3
- [7] Dan Hendrycks and Kevin Gimpel. A baseline for detecting misclassified and out-of-distribution examples in neural networks. *arXiv preprint arXiv:1610.02136*, 2016. 6
- [8] Junkai Huang, Chaowei Fang, Weikai Chen, Zhenhua Chai, Xiaolin Wei, Pengxu Wei, Liang Lin, and Guanbin Li. Trash to treasure: Harvesting ood data with cross-modal matching for open-set semi-supervised learning. In *Proceedings of the IEEE/CVF International Conference on Computer Vision*, pages 8310–8319, 2021. 2, 6
- [9] Prannay Khosla, Piotr Teterwak, Chen Wang, Aaron Sarna, Yonglong Tian, Phillip Isola, Aaron Maschinot, Ce Liu, and Dilip Krishnan. Supervised contrastive learning. *Advances in neural information processing systems*, 33:18661–18673, 2020. 3, 4
- [10] Alex Krizhevsky, Geoffrey Hinton, et al. Learning multiple layers of features from tiny images. 2009. 6
- [11] Samuli Laine and Timo Aila. Temporal ensembling for semi-supervised learning. *arXiv preprint arXiv:1610.02242*, 2016. 4
- [12] Junnan Li, Pan Zhou, Caiming Xiong, and Steven CH Hoi. Prototypical contrastive learning of unsupervised representations. *arXiv preprint arXiv:2005.04966*, 2020. 2, 3
- [13] Zekun Li, Lei Qi, Yinghuan Shi, and Yang Gao. Iomatch: Simplifying open-set semi-supervised learning with joint inliers and outliers utilization. In *Proceedings of the IEEE/CVF International Conference on Computer Vision*, pages 15870–15879, 2023. 2, 6
- [14] Yuval Netzer, Tao Wang, Adam Coates, Alessandro Bissacco, Baolin Wu, Andrew Y Ng, et al. Reading digits in natural images with unsupervised feature learning. In *NIPS workshop on deep learning and unsupervised feature learning*, page 4. Granada, 2011. 6
- [15] Aaron van den Oord, Yazhe Li, and Oriol Vinyals. Representation learning with contrastive predictive coding. *arXiv preprint arXiv:1807.03748*, 2018. 4
- [16] Kuniaki Saito and Kate Saenko. Ovanet: One-vs-all network for universal domain adaptation. In *Proceedings of the IEEE/CVF international conference on computer vision*, pages 9000–9009, 2021. 2, 5
- [17] Kuniaki Saito, Donghyun Kim, and Kate Saenko. Openmatch: Open-set semi-supervised learning with open-set consistency regularization. *Advances in Neural Information Processing Systems*, 34:25956–25967, 2021. 1, 2, 5, 6
- [18] Kihyuk Sohn, David Berthelot, Nicholas Carlini, Zizhao Zhang, Han Zhang, Colin A Raffel, Ekin Dogus Cubuk, Alexey Kurakin, and Chun-Liang Li. Fixmatch: Simplifying semi-supervised learning with consistency and confidence. *Advances in neural information processing systems*, 33:596–608, 2020. 5
- [19] Laurens Van der Maaten and Geoffrey Hinton. Visualizing data using t-sne. *Journal of machine learning research*, 9(11), 2008. 7
- [20] Erik Wallin, Lennart Svensson, Fredrik Kahl, and Lars Hammarstrand. Improving open-set semi-supervised learning with self-supervision. In *Proceedings of the IEEE/CVF Winter Conference on Applications of Computer Vision*, pages 2356–2365, 2024. 2
- [21] Erik Wallin, Lennart Svensson, Fredrik Kahl, and Lars Hammarstrand. Prosub: Probabilistic open-set semi-supervised learning with subspace-based out-of-distribution detection. In *European Conference on Computer Vision*, pages 129–147. Springer, 2024. 2, 6
- [22] Yidong Wang, Hao Chen, Yue Fan, Wang Sun, Ran Tao, Wenxin Hou, Renjie Wang, Linyi Yang, Zhi Zhou, Lan-Zhe Guo, et al. Usb: A unified semi-supervised learning benchmark for classification. *Advances in Neural Information Processing Systems*, 35:3938–3961, 2022. 6
- [23] Zerun Wang, Liuyu Xiang, Lang Huang, Jiafeng Mao, Ling Xiao, and Toshihiko Yamasaki. Scmatch: Alleviating overtrusting in open-set semi-supervised learning. In *European Conference on Computer Vision*, pages 217–233. Springer, 2024. 2
- [24] Zhirong Wu, Yuanjun Xiong, Stella X Yu, and Dahua Lin. Unsupervised feature learning via non-parametric instance discrimination. In *Proceedings of the IEEE conference on computer vision and pattern recognition*, pages 3733–3742, 2018. 3
- [25] Fisher Yu, Ari Seff, Yinda Zhang, Shuran Song, Thomas Funkhouser, and Jianxiong Xiao. Lsun: Construction of a

- large-scale image dataset using deep learning with humans in the loop. *arXiv preprint arXiv:1506.03365*, 2015. [6](#)
- [26] Qing Yu, Daiki Ikami, Go Irie, and Kiyoharu Aizawa. Multi-task curriculum framework for open-set semi-supervised learning. In *Computer Vision—ECCV 2020: 16th European Conference, Glasgow, UK, August 23–28, 2020, Proceedings, Part XII 16*, pages 438–454. Springer, 2020. [1](#), [2](#), [6](#)
- [27] Sergey Zagoruyko. Wide residual networks. *arXiv preprint arXiv:1605.07146*, 2016. [6](#)